REVISION 1.

Phosphate-halogen Metasomatism of Lunar Granulite 79215: Impact-induced Fractionation of Volatiles and Incompatible Elements

Allan H. Treiman[1], Jeremy W. Boyce[2], Juliane Gross[3], Yunbin Guan[2], John M. Eiler[2], and Edward M. Stolper[2].

[1] Lunar and Planetary Institute, 3600 Bay Area Boulevard, Houston TX 77058-1113. treiman@lpi.usra.edu

[2] Division of Geological & Planetary Sciences, California Institute of Technology, 1200 E. California Blvd., Pasadena CA 91125.

[3] Department of Earth and Planetary Sciences, American Museum of Natural History, Central Park West at 79th Street, New York NY 10024.

ABSTRACT

In the last decade, it has been recognized that the Moon contains significant proportions of volatile elements (H, F, Cl), and that they are transported through the lunar crust and across its surface. Here, we document a significant segment of that volatile cycle in lunar granulite breccia 79215: impact-induced remobilization of volatiles, and vapor-phase transport with extreme elemental fractionation. 79215 contains ~1% volume of fluorapatite, $Ca_5(PO_4)_3(F,Cl,OH)$, in crystals to 1 mm long, which is reflected in its analyzed abundances of F, Cl, and P. The apatite has a molar F/Cl ratio of ~10, and contains only 25 ppm OH and low abundances of the rare earth elements (REE). The chlorine in the apatite is isotopically heavy, at $\delta^{37}Cl$=+32.7±1.6‰. Hydrogen in the apatite is heavy at δD=+1060±180‰; much of that D came from spallogenic nuclear reactions, and the original δD was lower, between +350‰ and +700‰. Unlike other P-

rich lunar rocks (e.g., 65015), 79215 lacks abundant K and REE, and other igneous incompatible elements characteristic of the lunar KREEP component. Here, we show that the P and halogens in 79215 were added to an otherwise 'normal' granulite by vapor-phase metasomatism, similar to rock alteration by fumarolic exhalations as observed on Earth. The ultimate source of the P and halogens was most likely KREEP, it being the richest reservoir of P on the Moon, and 79215 having H and Cl isotopic compositions consistent with KREEP. A KREEP-rich rock was heated and devolatilized by an impact event. This vapor was fractionated by interaction with solid phases, including merrillite (a volatile-free phosphate mineral), a Fe-Ti oxide, and a Zr-bearing phase. These solids removed REE, Th, Zr, Hf, etc. from the vapor, and allowed the vapor to transport primarily P, F, and Cl, with lesser proportions of Ba and U into 79215. Vapor-deposited crystals of apatite (to 30 μm) are known in some lunar regolith samples, but lunar vapor has not (before this) been implicated in significant mass transfer. It seems unlikely, however, that phosphate-halogen metasomatism is related to the high Th/Sm abundance ratios of this and other lunar magnesian granulites. The metasomatism of 79215 emphasizes the importance of impact heating in the lunar volatile cycle, both in mobilizing volatile components into vapor and in generating strong elemental fractionations.

KEYWORDS: lunar, apatite, volatiles, metasomatism, Apollo 79215.

INTRODUCTION

The recent finds of relatively abundant water in lunar materials and on its surface have spiked interest in the origins and histories of lunar volatiles (Feldman et al. 2001; Saal et al. 2008, 2013; Pieters et al. 2009; Boyce et al. 2010; McCubbin et al. 2010a,b; Greenwood et al. 2011; Hauri et al. 2011; Liu et al. 2012). However, the overall abundance of volatile species in the Moon is controversial (e.g., Sharp et al. 2010; Paniello et al. 2012). The mineral apatite, $Ca_5(PO_4)_3(OH,F,Cl)$, is widespread among lunar samples (Meyer 2012), and has been central to studies of lunar volatiles as an indicator of their absolute and relative abundances, and the isotopic compositions of H and Cl (Boyce et al. 2010, 2013; McCubbin et al. 2010a,b, 2011; Sharp et al. 2010; Greenwood et al. 2011, 2012; Tartese and Anand 2013; Tartese et al. 2013).

Recent studies have emphasized the abundances and origins of lunar volatile species (and their unusual isotopic characteristics), but the recognition that volatile constituents are widespread on the Moon suggests the possibility that volatile-mediated mass transfers and chemical fractionations could also be widespread. The best-known lunar example of volatile-mediated mass transfers, 'rusty rock' 66095, is unique (Hunter and Taylor 1981; Shearer et al. 2012a; Burger et al. 2013; Provencio et al. 2013), and S-rich vapors have been implicated in sulfidation of some lunar breccias (Shearer et al. 2012b). In addition, one group of lunar rocks, the magneisan granulites, shows chemical fractionations that cannot be ascribed easily to silicate igneous processes (Korotev and Jolliff 2001; Korotev et al. 2003; Treiman et al. 2010). In general, these granulites have unfractionated REE patterns (i.e., abundance ratios like CI chondrites), but have Th/Sm ratios far above what could be expected from silicate igneous

fractionation (i.e., in the most fractionated lunar component, KREEP: Warren and Wasson 1979; Jolliff 1999).

Lunar sample 79215 is at the intersection of these two issues – it contains apatite in abundance, and is one of the magnesian aluminous granulites with a high Th/Sm ratio (Bickel et al. 1976; McGee et al. 1978; Hudgins et al. 2008). 79215 was collected as a loose rock on the lunar surface, near the rim of a subdued crater southeast of the prominent crater Van Serg (Muehlberger et al. 1973). In that area, many rocks have a distinctly lighter tone, and 79215 was among the largest of them (Fig. 224 in Muehlberger et al. 1973). It may be related to light-tone rocks exposed in the bottom of Van Serg crater, possibly from beneath the dark polymict regolith breccia that is abundant in the Van Serg ejecta (e.g., sample 79225). The physical orientation of 79215 is known from photography, and its original upper surface shows many scars of small meteoroid impacts ('zap pits,' Meyer 2012). 79215 has been analyzed extensively for petrography and chemistry, beginning with Bickel et al. (1976), Blanchard et al. (1977), and McGee et al. (1978); most recently Hudgins et al. (2008, 2011) have revisited the earlier analyses with modern methods.

The focus of this paper is a striking geochemical anomaly in 79215 – it is strongly enriched in phosphorus at ~200xCI (from its abundance of the mineral apatite), but has REE abundances at only moderate levels, ~ 10xCI; e.g., its P/Sm ratio is ~20. No other lunar sample shows such extreme fractionation among KREEP elements (which are normally quite coherent; Jolliff 1999), and demands explanation. Similarly, 79215 is anomalous in having Th/Sm ratio of ~3, or twice that in KREEP. To understand the origin of these geochemical anomalies, we have re-examined the petrography and mineral chemistry of 79215, obtained new chemical and stable isotopic analyses of its apatite, and re-evaluated its bulk composition. We examine the likelihood

that lunar volatiles were involved in creating these anomalies, and suggest that these processes may be widespread in the formation of lunar granulites.

SAMPLES AND METHODS

Samples

We studied thin sections 79215,51 and 79215,56 – both loaned by the Lunar Sample Curator, Johnson Space Center. In addition, we used X-ray maps of thin section 79215,76 provided by K. Joy.

Electron Microprobe Analyses

Major element chemical compositions of silicate and oxide minerals were obtained with the SX-100 electron microprobes at the Johnson Space Center, Houston TX and at the American Museum of Natural History, New York (Table 1). Analyses used standard procedures: wavelength dispersive spectrometry, accelerating potential of 15 kV, and beam current of 10 nA (Faraday cup). Standards included well-tested minerals and synthetic phases. Silicate mineral compositions appear to be fairly homogeneous across the analyzed thin section, see Deposit Item 2 (Bickel et al. 1976; McGee et al. 1978; Hudgins et al. 2011). Compositions of chromian spinels vary widely within and among thin sections (Bickel et al. 1976; McGee et al. 1978).

The chemical composition of apatite in 79215,51 was obtained using the SX-100 electron microprobe at the American Museum of Natural History, following the method of Goldoff et al. (2012). Analyses were obtained on volumes that had not experienced prior electron beam irradiation. Sodium and F were analyzed first, with a defocused beam at 10 kV accelerating potential and 4 nA beam current (Faraday cup). Then, other elements were analyzed at 15 kV and 20 na beam current. Standards included well-characterized natural and synthetic materials, including: berlinite (P), wollastonite (Ca), , MgF_2 (F), boracite (Cl),,diopside (Si, Mg), K-

feldspar (Al, K), olivine (Fe), jadeite (Na), rutile (Ti), rhodochrosite (Mn), troilite (S), and $CePO_4$ (Ce). Data quality was ensured by analyzing standard materials as unknowns. Apatite analyses were screened for off-totals (<99% and >100.5%), and for multiple percent-levels of SiO_2, Al_2O_3, FeO, and/or MgO, such as would indicate that the analysis volume included other phases. The chemical compositions of the 64 spots in 6 apatite grains are all within uncertainty of each other (see , and a single average composition is given in Table 2. Microprobe analyses of all phases are given in the Deposit Materials.

SIMS

Elemental abundances and isotopic compositions of Cl and H, and S in the apatite of 79215,51 were analyzed by secondary ion mass spectrometry, using the Cameca 7f-GEO at Division of Earth and Planetary Sciences, the California Institute of Technology; data are given in Table 3. Samples and standards were coated with ~ 30 nm of carbon to improve electrical conductivity, which did not permit analyses of abundances or isotopic composition of C (gold coating was not permitted on these lunar thin sections). Analytical procedures followed those of Boyce et al. (2010). Analyses were done at mass resolutions of $\Delta M/M$ ~5700, sufficient to separate $^{16}O^{1}H^{-}$ from $^{17}O^{-}$, $^{31}P^{1}H^{-}$ from $^{32}S^{-}$, and $^{35}Cl^{-}$ from $^{19}F^{16}O^{-}$. Hydrogen abundances were measured via the ion ratio $^{16}O^{1}H^{-}/^{17}O^{1-}$. Standards for all analyses were three terrestrial apatites (McCubbin et al. 2010; Boyce et al. 2012), San Carlos olivine (as a zero standard), with blanks in individual thin sections determined by analyzing olivine and plagioclase adjacent to the apatite grains in 79215. We did not analyze areas with obvious cracks (see Greenwood et al. 2011), and we rejected analyses with high H abundances, as likely representing contamination with epoxy or other materials. Full results of SIMS analyses are in Electronic Annex 1. The apatite grains have the same compositions, chemical and isotopic, across the whole thin section (Table 1, Online

Appendices). Average elemental abundances in the 79215 apatites, by SIMS, are: H_2O = 25 ppm ± 15 ppm (2σ); Cl = 8300 ppm ± 400 ppm (2σ); and S = 106 ppm ± 8 ppm (2σ). The abundance of Cl by SIMS is greater than that by EMP (6600 ppm, Table 2); the source of this discrepancy is not clear, but does not affect our discussions and conclusions. The average isotopic compositions measured here for 79215 apatites are: δD = +1060‰ ± 180‰ (2σ); $\delta^{\square\square}$Cl = +32.7‰ ± 1.6‰ (2σ); $\delta^{\square 3}$S = +5.5‰ ± 3.6‰ (2σ); and $\delta^{\square 4}$S = +10.5‰ ± 3.0‰ (2σ).

The apatite of 79215 contains so little hydrogen that spallogenic production of D, dominated by interaction of galactic cosmic rays with ^{16}O, has modified the δD value significantly. The H_2O abundance in the 79215 apatite is ~25 ppm, which is ~2.8 ppm H. With an analyzed δD of +1060‰ (Table 3), the abundance of D in the 79215 apatite is $(3.2\cdot10^{-4}$ moles-D/mole-H)*$(2.8\cdot10^{-6}$ moles-H/gram) = $9.0\cdot10^{-10}$ moles-D/gram. The rate of D production by spallogenesis from galactic cosmic rays is $0.92\cdot10^{-10}$ moles-D/gram·10^8years (Reedy 1982), and the exposure age of 79215 is ~$3\cdot10^8$ years (Meyer 2012). Thus, the total spallogenic D over time is $2.8\cdot10^{-10}$ moles-D/gram, or approximately one third of D analyzed in the 79215 apatite. Considering the uncertainty in the apatite H abundance, it is reasonable that ~1/3 – 2/3 of the D in 79215 apatite is from spallation, implying that the original, pre-spallogenesis apatite would have had δD = +350‰ to +700‰.

PETROGRAPHY & MINERALOGY

Apollo sample 79215 is a feldspathic granulite, annealed and chemically equilibrated; the protolith of this high-grade rock was a polymict impact melt breccia (Bickel et al. 1976; McGee et al. 1978; Hudgins et al. 2008), which last equilibrated at ~ 3.9 Ga (Oberli et al. 1979; Hudgins et al. 2008). 79215 is relatively rich in siderophile elements consistent with a CM-like meteoritic component (Higuchi and Morgan 1975; Fischer-Gödde et al. 2012). Approximately one quarter

157 of the rock is clasts of granoblastic-textured material rich in plagioclase and olivine, with longest
158 grain dimensions to 1 mm. The clasts are distinct from the surrounding matrix in grain size
159 (matrix grains <100 μm across) and texture (equant grains with boundary angles at ~120°).
160 79215 consists of ~80% plagioclase (An_{93}; Table 1; $An_{92\text{-}96}$; Meyer 2012), ~10% olivine ($Fo_{72.7}$),
161 ~4% low-Ca pyroxene ($Wo_{3.5}En_{73.5}Fs_{23}$), ~3% augite ($Wo_{42}En_{46}Fs_{11}$), and ~1% apatite (Table 1,
162 2), with ~0.5% chromite and ilmenite, and ~0.1% troilite (FeS) and low-Ni iron metal (Bickel et
163 al. 1976; McGee et al. 1978; Table 1). No merrillite has been reported. Pyroxene compositions
164 are consistent with equilibration at ~1000°C (Hudgins et al. 2011), and their Al and Ti contents
165 (Table 1) imply equilibration at low pressure (Nekvasil et al. 2004).
166 79215 contains ~1% apatite by volume, whereas typical lunar feldspathic granulites are
167 reported to contain no phosphate minerals or only trace proportions of them (Table 4). Apatite in
168 79215 occurs as grains ranging from millimeter-sized euhedra and subhedra (Fig. 1) down to
169 micron-sized anhedra in the matrix grains (like those in other feldspathic granulites). Larger
170 apatite grains commonly contain inclusions of plagioclase and olivine that are chemically
171 indistinguishable from those elsewhere in the rock. The apatite is not distributed randomly nor is
172 it concentrated in specific clasts or with specific other minerals (Fig. 1); rather it is concentrated
173 along curvilinear traces that crosscut the rock, mostly (but not exclusively) through matrix
174 material (Fig. 1).
175 Electron microprobe and SIMS analyses here show that the apatite is chemically
176 homogeneous fluorapatite (Table 2) with molar F/Cl ≈ 10 and molar OH/(OH+F+Cl) ≈ 0.013 (by
177 difference & stoichiometry), equivalent to ~450 ppm (weight) H_2O, which is within uncertainty
178 of zero. SIMS analyses here give H_2O = 25±15 ppm 2σ (Table 3), which is isotopically heavy at
179 δD = +1060±180‰ 2σ (Table 3). As described above, much of the D is likely to be from

spallation from ^{16}O by galactic cosmic rays, implying a pre-spallation $\delta D = \sim+700 - \sim+350‰$. Chlorine in the apatite is also isotopically heavy, $\delta^{37}Cl = +32.7 \pm 1.6‰$ 2σ. These δD and $\delta^{37}Cl$ values are typical of lunar materials, including KREEP-rich basalts and highlands rocks (Sharp et al. 2010; Boyce et al. 2010, 2013; Greenwood et al. 2011, 2012; Robinson et al. 2013). Sulfur in the apatite has $\delta^{33}S = +5.5 \pm 3.6‰$ and $\delta^{34}S = +10.5 \pm 3.0‰$ (2σ), consistent with mass-fractionation from chondritic sulfur ($\delta^{33}S = \delta^{34}S = 0‰$), and similar to values measured in some lunar regolith samples and regolith breccias (Rees and Thode 1974; Sharp et al. 2010; Shearer et al. 2012a).

CHEMISTRY AND ORIGIN

79215 is remarkable for its high abundance of apatite, reflected in its high abundances of P and halogens relative to otherwise comparable feldspathic granulites (Fig. 2a; Table 4; Bickel et al. 1976; Meyer 2012), without comparable enrichments of other KREEP elements (e.g., REE, Th). This excess of P and halogens, and the apatite's arrangement on curvilinear traces (see above and Fig. 1), suggest that constituents of the apatite were added to a feldspathic granulitic protolith by a fluid phase that penetrated along cracks, and that the apatites record the passage of this fluid.

Elemental abundances in 79215 are mostly as compiled in the Lunar Sample Compendium (Meyer 2012) from Bickel et al. (1976), McGee et al. (1978), and Hudgins et al (2008). The abundance of P in 79215 has been reported only once before, as calculated from the modal abundances of apatite in one section (McGee et al. 1978); our report of P abundances is also based on modal abundance of apatite, but on the average of eleven thin sections reported here and in the literature, and our chemical analysis of apatite (Table 2). Abundances of F and Cl

are calculated from our chemical analysis of apatite (Table 2), and its average modal abundance of 1%, Table 4).

The lunar KREEP component (Warren and Wasson 1979; Jolliff 1999) is the plausible ultimate source of the P, F, and Cl in 79215; it is the only known lunar reservoir rich in P and contains significant F and Cl (Electronic Annex 2). Such a KREEP-rich source is consistent with the apatite's anion composition (i.e., molar F/Cl ≈10 and low H; Table 1; McCubbin et al. 2012). The high δD and δ^{37}Cl of 79215 are also consistent with the characteristics of KREEP (Sharp et al. 2010; Boyce et al. 2013; Greenwood et al. 2012; Robinson et al. 2013), although this association is not as clear in highlands rocks as in mare basalts (Boyce et al. 2013). However, despite these features that are consistent with a connection to KREEP, 79215 is not strongly enriched in other elements characteristic of KREEP, including the REE, U, Th, Ta, Zr, K, and Ba (Fig. 2b; Electronic Annex 2). Thus, if the P and halogen atoms in the 79215 apatite were ultimately derived from KREEP, significant elemental fractionations must have occurred in the processes of extraction, transport, and/or deposition into 79215.

Elemental Fractionation Scenarios

Without a geological context for 79215, we cannot establish which of several possible scenarios may have led to its strong elemental fractionations relative to other feldspathic granulites and to KREEP. Although it is reasonable that 79215 was metasomatized by a fluid derived from a KREEPy source, the fluid's history and composition are not tightly constrained. Significantly, there are no direct constraints on the fates of elements usually present in KREEPy material but not enriched in 79215 (Figure 2); we cannot tell if the metasomatic fluid did not contain significant enrichments in these elements in the first place, deposited these elements elsewhere before it interacted with 79215, or carried the elements through 79215 toward some

other final destination.

The simplest scenario for most elements is the first: the elemental enrichments in 79215 were inherited from the metasomatic agent and directly reflect its composition as it exited a KREEP-bearing source; i.e., the elements in this fluid were quantitatively added to 79215 as the fluid passed through it. The task then is to understand how some elements known to be abundant in KREEP were significantly depleted relative to P, F, and Cl in the metasomatic agent; i.e. what could have led them to be retained in the KREEP-bearing source area? A simple explanation would be that these elements were retained in residual crystalline phases with low fluid/mineral partition coefficients, resulting in a P-Cl-F-rich fluid that is depleted in Th, REE, Ta, Zr, and Hf (Fig. 2b). Equilibration of fluid with an assemblage of residual phases that included merrillite, a Zr-rich phase such as zircon, a Ti (-Fe) oxide, and some alkali feldspar or 'K-fraction' late immiscible liquid (Neal and Taylor 1989, 1991; Jolliff 1999), in addition to plagioclase, olivine, and pyroxenes, could qualitatively generate a fluid that is depleted in REE, U, Th, Ta, Zr, K and Ba relative to P, Cl, and F; relevant partition coefficients are tabulated in Electronic Annex 3. This mineral assemblage is in fact present in KREEP basalts (Ryder and Bower 1976; Ryder and Martinez 1976). The inferred similar enrichments in Cl and F in the metasomatic fluid relative to KREEP (Fig. 2b) suggest that the residue contained little F or Cl, and thus no apatite; but the inferred depletion in the fluid of P relative to Cl and F compared to KREEP (Fig. 2b, see Electronic Annex 2) is consistent with the presence in the residue of a significant amount of merrillite. Residual merrillite would retain REE nearly completely; it would also retain Th relative to U (Electronic Annex 3; Benjamin et al. 1978; Crozaz 1979). The low abundances of Zr and Hf could be explained by residual zircon or other Zr-rich phase (e.g. badelleyite ZrO_2 or zirconolite $CaZrTi_2O_7$) in the residua. The low abundance of Ta could likely be explained by

248 residual rutile, ilmenite, or armalcolite (Schmidt et al. 2004; Klemme et al. 2006; Dygert et al.
249 2013). The low abundances of K and Ba could be explained by residual alkali feldspar or an
250 immiscible 'K-fraction' melt derived from KREEP (Neal and Taylor 1989, 1991; Jolliff 1999).
251 A more complex but probably more reasonable scenario is that of reactive transport – that
252 the metasomatic fluid evolved as it moved to and through 79215 (Korzhinski 1965; Steefel and
253 Maher 2009), and that it had carried elements that were not deposited in 79215. In this scenario,
254 for instance, a fluid generated from a KREEP-rich rock might contain a wide range of KREEP
255 elements, for instance like the immiscible 'REEP-fraction' melt (Neal and Taylor 1989, 1991;
256 Jolliff 1999), and deposit minerals like zircon, rutile, and merrillite *en route* to the protolith of
257 79215. Deposition of zircon and rutile would deplete the fluid in Zr, Hf, and Ta; deposition of
258 merrillite would deplete the fluid in REE and Th, P and U. Later, the fluid's remaining P would
259 combine with much of its Cl and F in the 79215 protolith to deposit apatite. The Ca to form
260 apatite could have been carried in the fluid (McKay et al. 1972) or come from decomposition of
261 augite in the protolith (e.g., via $CaMgSi_2O_6 + Mg_2SiO_4 \Rightarrow CaO_{(fluid)} + 3\ MgSiO_3$). Other KREEP
262 elements, like Cs and Li, might have passed through the 79215 protolith to be deposited (or
263 dispersed) elsewhere.

264 **Metasomatic Agent**

265 The nature of the agent that transported P, Cl, and F to 79215 is of interest, because
266 processes involving fluids (other than silicate melts) are rarely evident in lunar rocks (Shearer et
267 al., 2011). The chemical signature of metasomatism in 79215 and the textures of its apatite are
268 most consistent with transport by a halogen-rich vapor phase such as has been documented in the
269 lunar regolith (McKay et al. 1972) and in terrestrial deposits like the source of Durango apatite
270 (Lyons 1988).

Other types of metasomatic agents seem unlikely. On Earth, metasomatism is commonly ascribed to aqueous or carbonic fluids, but (despite recent evidence that the Moon is not as dry as had generally been believed and that C-bearing gases exsolve from mare basalts during eruption; Sharp et al. 2010; McCubbin et al. 2010; Nicholis and Rutherford 2009) we know of no evidence for such fluids on the Moon, which is generally at redox states too reduced for abundant H_2O or CO_3 (McGee et al. 1978; Zhang 2011). Sulfidic liquid or vapor has been invoked to account for some altered rocks (Shearer et al. 2011), but 79215 contains little sulfide and no evidence that sulfides have replaced other minerals.

Silicate melts can act as metasomatic fluids, and the pyroxene equilibration temperature for 79215 (~1000°C) is high enough that one could expect formation (or existence) of a silicic or intermediate-composition silicate melt. However, silicate melt is unlikely because it cannot carry enough phosphorus: P_2O_5 solubility is only ~6% in basaltic melt and ~3% in intermediate melt (Watson 1979). To put 1% apatite into 79215 would require that ~8% (mass) of the rock be basaltic melt, or ~17% intermediate melt, and these amounts are not apparent in either rock chemistry or texture (e.g., vein-like bodies richer in mafic minerals than the host feldspathic granulite).

Silicate melt is also unlikely because it cannot account for the fractionations required for the mixing model of Figure 2c. If the event that enriched 79215 in P, Cl, and F acted on other KREEP elements in the same way, the rock would contain all other KREEP elements at ~0.5 times KREEP itself (Jolliff 1999). However, 79215 actually contains only 0.01 times KREEP abundances of REE, U, Th, Hf, Zr, and Ta (Figure 2b), which is the abundance level of typical feldspathic granulites (e.g., 78155). Therefore, whatever processes acted to produce the metasomatic fluid caused those latter elements to be fractionated by a factor of >50 (i.e.,

0.5/0.01). For the REE and Th, this is not possible in single-stage fractionation of a silicate melt that equilibrated with merrillite, because $^{REE}D_{merrillite/melt} < 10$ for REE-rich systems like a KREEPy source (Jolliff et al. 1993). In effect, silicate melts are too good as solvents for the REE. Greater fractionations could arise from multiple fractionation events (or continuous fractionations as in chromatographic separations); these complicated scenarios cannot be ruled out, but there is no evidence in their favor.

Phosphate-rich melts are known as products of late-stage liquid immiscibility in siliceous melt systems and can (obviously) carry significant phosphorus and halogens (Tacker and Stormer 1993). Phosphate-rich melts have been hypothesized in evolved KREEP-rich systems as products of liquid immiscibility – separation of a highly polymerized K-rich silicate melt (the 'K-fraction') from an unpolymerized silicate-phosphate melt (the 'REEP-fraction'), which could then carry the 'REEP' signature into other highland rocks (Jolliff 1999; Neal and Taylor 1989, 1991). However, the REEP-fraction melts share the same problem described above as do common silicate melts; they cannot support the fractionations required for the mixing model of Figure 2c (Jolliff et al. 1993).

Halide melts also seem unlikely, as they have not been reported in lunar samples or in experiments on lunar systems. To our knowledge, however, there has been no search for traces of halide melts in lunar samples and few relevant experimental studies.

We conclude that vapor transport is the most plausible mechanism for metasomatism of 79215. Metasomatism by vapor transport has been proposed to account for enrichments in volatile elements in samples like 66095 (Hunter and Taylor 1981) and for sulfidation of some breccias (Shearer et al. 2012a). In several samples of lunar regolith, apatite (and thus its constituent P and halogens) was deposited from vapor (McKay et al. 1972; Ruzicka et al. 2000;

Davis et al. 2001); SEM imagery of sample 14261 (McKay et al. 1972) is particularly compelling. In some cases, the REE were also transported along with P and halogens (Davis et al. 2001). Vapor transport has also been invoked to explain the distributions of P in and among meteoritic basalts (Davis et al. 2001; Mittlefehldt 1987; Barrat et al. 2009; Shearer et al. 2011), and implicated in transport of REE and high field strength elements (HFSE, including U, Th, and Ta) in some terrestrial rocks (de Hoog and van Bergen 2000; Salvi and Williams-Jones 2006). 79215 is also enriched in some highly volatile elements, including Zn, Se, Ag, Br, and Te (Higuchi and Morgan 1975); these elements could conceivably have been transported into 79215 by metasomatic fluid.

Constraints on Vapor Composition

The metasomatic vapor that affected 79215 acted under low confining pressures (i.e., was not a liquid or supercritical fluid). Its composition is poorly constrained, because we lack ways to measure absolute pressure, or partial pressures of the gases most likely to be abundant, including CO, CO_2, and H_2. However, the vapor must carry significant P, Cl, and F, be poor in reduced sulfur species, and be reduced enough to coexist with iron-rich metal. Equilibria among minerals in 79215 do permit one to constrain oxygen fugacity, sulfur fugacity, and thereby fugacity ratios of H_2/H_2O, CO/CO_2, and S_2/SO_2. Given the high equilibration temperature of ~1000°C (Hudgins et al. 2011) and the inference of low pressure (the rock being in an ejecta blanket), we can take fugacity (from thermochemical calculations) as equivalent to gas partial pressure.

The oxidation state of 79215 is constrained by mineral reactions to a low oxygen fugacity, $f(O_2)$, comparable to those of most lunar rocks. The dominant oxygen buffer is the equilibrium Fe_2SiO_4(olivine) = $FeSiO_3$(pyroxene) + Fe^0(metal) + ½ O_2(gas). For pure minerals, this reaction lies ~0.2 log unit $f(O_2)$ below the iron-quartz-fayalite buffer, IQF, at 1000°C (from

the THERMOCALC code; Holland and Powell 2011). Assuming site-by-site ideal mixing in olivine and orthopyroxene (Table 1) and the metal composition of McGee et al. [1978] one calculates that this equilibrium is displaced ~0.5 log units toward more reducing conditions, i.e. to $\log[f(O_2)] \approx$ IQF – 0.7 or iron-wüstite (IW) – 1.7. Limiting reactions involving breakdown of ilmenite and absence of armalcolite are consistent with this value, and require $\log[f(O_2)]$ between IQF and IQF – 1 (cited as 1 to 2 log units of $f(O_2)$ below IW; McGee et al. 1978). This oxidation state is consistent with the presence of apatite and Fe metal (Nash and Hausel 1973).

At such low oxygen fugacity, the metasomatizing vapor must be relatively poor in H_2O and in CO_2. The molar ratio H_2/H_2O must have been ~5 under these conditions (Zhang 2011), suggesting that little H_2O and thus OH were available to form hydroxyapatite. This predicted dearth of OH is consistent with the analyzed composition (Table 2; Table EA 1a). Similarly, the molar ratio CO/CO_2 must have been ~13 (calculated from tabulated thermochemical data of Robie and Hemingway 1995). The fugacity of S_2 in 79215 is constrained by the presence of Fe metal and FeS (troilite) by the equilibrium $FeS = Fe + ½ S_2$. For 1000°C, this equilibrium buffers $\log[f(S_2)]$ to ~ 10^{-7} bars (thermochemical data from Robie and Hemingway 1995). The abundance of SO_2 gas is similar at $\log[f(SO_2)] \sim 10^{-8}$ bars, and that of SO_3 is vanishingly small.

The transporting vapor could have been composed dominantly of phosphorus halide and oxide species (e.g., PF_5, PO_2), or it could have included C-O-S species as inferred for lunar volcanic gases (Fegley 1991; Nicholis and Rutherford 2009) The vapor here was distinctly different from that recorded in sample 66095 (the 'rusty rock'), which was rich in halogens but which deposited P as Fe_3P (schreibersite) rather than as apatite or merrillite (Hunter and Taylor 1981). The difference between these two metasomatic products (79215 and 66095) could reflect different blocking temperatures (Yakovlev et al. 2006) or gas compositions (Fegley 1991).

Implications

Lunar rock 79215 records a lunar metasomatic event in which significant proportions of halogens (Cl and F) and phosphorus, with lesser K, Ba, and U, were transferred from a KREEP-rich source without large transfers of REE, Th and other KREEP elements. While 79215 is apparently unique among returned samples in showing extensive F-Cl-P metasomatism, vapor-deposited apatite is found on the surfaces of lunar regolith grains (McKay et al. 1972). This metasomatic event is consistent, in general, with fractionation of an original KREEPy source containing merrillite + zircon + a Fe-Ti-oxide + alkali feldspar; the fractionated fluid then deposited into 79215 abundant halogens and phosphorus, and small proportions of K, U, Th, and Ba.

This vapor transport metasomatism was related to and probably induced by the impact event that assembled 79215 as a breccia and heated it to allow annealing. One can imagine a hot ejecta blanket cooking regolith and rock beneath it, and thus mobilizing its volatiles, as has been envisioned for basalt flowing over regolith (Rumph et al. 2013). In this sense, the metasomatism of 79215 can be compared to chemical alteration near a fumarole, as is commonly observed (both actively and as fossil deposits) in terrestrial ash-flow tuffs and ejecta blankets, and has been inferred from the morphology of some martian ejecta blankets (Tornabene et al. 2012). Fumarolic alteration has also been invoked for lunar sample 66095 (Shearer et al. 2012b), the "rusty rock," although its alteration differs from that of 79215 in being marked by deposition of $FeCl_2$ and Fe_3P (Hunter and Taylor 1981). 66095 also contains the volatile-free phosphate stanfieldite, $Ca_4(Mg,Fe)_5(PO_4)_6$, which is interpreted as a reaction product between Fe-Ni-P metal and Ca-bearing silicates (Burger et al. 2013). Apatite is not present in the 66905 alteration materials.

Rock 79215 is also enriched in Th relative to Sm, with a Th/Sm ratio significantly above KREEP (Fig. 3, but not obvious in Fig. 2). Could this high Th/Sm ratio also have been established in halogen-phosphate metasomatism? To produce a high Th/Sm ratio using the model of residual merrillite described above, one must invoke an effective $^{Th/Sm}D_{merrillite/fluid} < 1$, so that more Sm than Th is retained in the residual merrillite. Relevant partition coefficients are given in Electronic Annex 3, from which one can estimate that $^{Th/Sm}D_{merrillite/melt} \approx 0.9$ with large uncertainty; this value is based on single-element partition coefficients in different bulk compositions and physical conditions. In very broad terms, this D value is not consistent with generation of a high Th/Sm ratio via phosphate-halogen metasomatism, and the high Th/Sm would reflect some other fractionation process. Many other lunar granulites have Th/Sm above that of KREEP (Fig. 3; Korotev and Jolliff 2001; Korotev et al. 2003), giving broader applicability to the question of halogen-phosphate metasomatism in granulites. Because of the uncertainties in relevant partition coefficients (Electronic Annex 3), it is clear that more work is needed.

The metasomatism of 79215 thus represents a previously unrecognized process in the lunar volatiles cycle – impact induced devolatilization of KREEPy material, and transfer of volatiles rich in phosphate and halogens. 79215 became enriched in P, F, and Cl, but not in more volatile elements like Zn and Cd. Perhaps these and other volatile species passed through 79215, eventually to form deposits like those in ‘rusty rock’ 66095 (Hunter and Taylor 1981). Some proportion of these volatiles would have passed through lunar rock and regolith (after reactions and fractionations) into the lunar atmosphere. From there, the volatile species could escape to space or return to the lunar surface, and from there be remobilized by heat, cosmic rays, or later other asteroidal and cometary impacts.

ACKNOWLEDGMENTS

We are grateful to: K. Joy and O. Abramov for the use of Figure 1; A. Peslier (JSC) for assistance with electron microprobe analyses; K. Joy, C. Neal, and B. Jolliff for useful comments; and {your names here} for helpful reviews. This work was supported in part by NASA Cosmochemistry Grant NNX12AH64G to AHT, and a subcontract to JG from the NASA Lunar Science Institute node at the LPI (contract NNA09DB33A: D.A. Kring, PI). Lunar and Planetary Institute Contribution #1xxx.

REFERENCES

Benjamin, T., Heuser, W.R., and Burnett, D.S. (1978) Laboratory studies of actinide partitioning revelant to ^{244}Pu chronometry. *Proceedings of the 9th Lunar and Planetary Science Conference*, 1393-1406.

Barnes, J.J., Franchi, I.A., Anand, M., Tartèse, R., Starkey, N.A., Koike, M., Sano, Y., and Russell, S.S. (2013) Accurate and precise measurements of the D/H ratio and hydroxyl content in lunar apatites using NanoSIMS. *Chemical Geology,* 337, 48-55.

Barnes, J.J., Tartèse, R., Anand, M., McCubbin, F.M., Franchi, I.A., Starkey, N.A., and Russell, S.S. (2014) The origin of water in the primitive Moon as revealed by the lunar highlands samples. *Earth and Planetary Science Letters,* 390, 244-252.

Barrat J.-A., Yamaguchi, A., Greenwood, R.C., Bollinger, C., Bohn, M., and Franchi, I.A. (2009) Trace element geochemistry of K-rich impact spherules from howardites. *Geochimica et Cosmochimica Acta,* 73, 5944-5958.

Bickel, C.E., Warner, J.L., and Phinney, W.C. (1976) Petrology of 79215: Brecciation of a lunar cumulate. *Proceedings of the Lunar and Planetary Science Conference 7th*, 1793-1819.

Blanchard, D.P., Jacobs, J.W., and Brannon, J.C. (1977) Chemistry of ANT -suite and felsite clasts from consortium breccia 73215 and of gabbroic anorthosite 79215. *Proceedings of the Lunar and Planetary Science Conference 8th*, 2507-2524.

Boyce, J.W., Liu, Y., Rossman, G.R., Guan, Y., Eiler, J.M., Stolper, E.M., and Taylor, L.A. (2010) Lunar apatite with terrestrial volatile abundances. *Nature,* 466, 466-469.

436 Boyce, J.W., Eiler, J.M., and Channon, M.B. (2012) An inversion-based self-calibration for
437 SIMS measurements: Application to H, F, and Cl in apatite. *American Mineralogist*, 97,
438 1116-1128.
439 Boyce, J.W., Guan, Y., Treiman, A.H., Greenwood, J.P., Eiler, J.M., and Ma, C. (2013) Volatile
440 components in the Moon: Abundances and isotope ratios of Cl and H in lunar apatites.
441 *Lunar and Planetary Science Conference 44th*, Abstr. #2851.
442 Burger, P.V., Shearer, C.K., Sharp, Z.D., McCubbin, F.M., Provencio, P., and Steele, A. (2013)
443 Driving fumarole activity on the Moon 1. Chlorine distribution and its isotope composition
444 in "rusty rock" 66095. Implications for the petrogenesis of "rusty rock," origin of "rusty"
445 alteration, and volatile element behavior on the Moon. *Lunar and Planetary Science*
446 *Conference* 44th, Abstract #2182.
447 Crozaz, G. (1979) Uranium and thorium microdistributions in stony meteorites. *Geochimica et*
448 *Cosmochimica Acta,* 43, 127-136.
449 Davis, A.M., Dufek, J.D., and Wadhwa M. (2001) Euhedral phosphate grains in vugs and
450 vesicles in ordinary chondrites, lunar samples and the Ibitira eucrite: Implications for trace
451 element transport processes. *Meteoritics and Planetary Science,* 36, A 47, Abstract #5284.
452 deHoog, J.C.M., and van Bergen, M.J. (2000) Volatile-induced transport of HFSE, REE, Th, and
453 U in arc magmas: Evience from zirconolite-bearing vesicles in potassic lavas of Lewotolo
454 volcano (Indonesia). *Contributions to Mineralogy and Petrology,* 139, 485-502.
455 Dygert, N., Liang, Y., and Hess P. (2013) The importance of melt TiO_2 in affecting major and
456 trace element partitioning between Fe–Ti oxides and lunar picritic glass melts. *Geochimica*
457 *et Cosmochimica Acta,* 88, 134-151.
458 Fegley, B.F.Jr. (1991) Thermodynamic models of the chemistry of lunar volcanic gases.
459 *Geophysical Research Letters,* 18, 2073-2076.
460 Feldman, W.C. et al. (2001) Evidence for water ice near the lunar poles. *Journal of Geophysical*
461 *Research*, 106, 23231-23251.
462 Fischer-Gödde, M., and Becker, H. (2012) Osmium isotope and highly siderophile element
463 constraints on ages and nature of meteoritic components in ancient lunar impact rocks.
464 *Geochimica et Cosmochimica Acta,* 77, 135-156.

Goldoff, B., Webster, J.D., and Harlov, D.E. (2012) Characterization of fluor-chlorapatites by electron probe microanalysis with a focus on time-dependent intensity variation of halogens. *American Mineralogist*, 97, 1103-1115.

Greenwood, J.P., Itoh, S., Sakamoto, N., Warren, P.H., Taylor, L.A., and Yurimoto, H. (2011) Hydrogen isotope ratios in lunar rocks indicate delivery of cometary water to the Moon. *Nature Geoscience,* 4, 79-82.

Greenwood, J.P., Itoh, S., Sakamoto, N., Warren, P.H., Taylor, L.A., and Yurimoto, H. (2012) Towards a wetter Moon: Implications of high volatile abundances in lunar apatite. *43rd Lunar and Planetary Science Conference*, Abstract #2089.

Hauri, E.H., Weinreich, T., Saal, A.E., Rutherford, M.C., and Van Orman, J.A. (2011) High pre-eruptive water contents preserved in lunar melt inclusions. *Science*, 333, 213-215.

Higulchi, H. and Morgan J.W. (1975) Ancient meteoritic component in Apollo 17 boulders. *Proceedings of the Lunar Science Conference 6th vol.* 1, 739-752.

Holland, T.J.B., and Powell, R. (2011) An improved and extended internally consistent thermodynamic dataset for phases of petrological interest, involving a new equation of state for solids. *Journal of Metamorphic Geology*, 29, 333-383.

Hubbard, N.J., Rhodes, J.M., Wiesmann, H., Shih, C.-Y., and Bansal, B.M. (1974) The chemical definition and interpretation of rock types returned from the non-mare regions of the Moon. *Proceedings of the Fifth Lunar Conference* (Supplement 5, *Geochimica et Cosmochimica Acta*) Vol. 2, 1227-1246.

Hudgins, J.A., Spray, J.G., Kelley, S.P., Korotev, R.C., and Sherlock, S.C. (2008) A laser probe $^{40}Ar/^{39}Ar$ and INAA investigation of four Apollo granulitic breccias. *Geochimica et Cosmochimica Acta,* 72, 5781-5798.

Hudgins, J.A., Spray, J.G., and Hawkes C.D. (2011) Element diffusion rates in lunar granulitic breccias: Evidence for contact metamorphism on the Moon. *American Mineralogist,* 96, 5781-5798.

Hunter, R.H., and Taylor, L.A. (1981) Rusty Rock 66095: A paradigm for volatile-element mobility in highland rocks. *Proceedings of Lunar and Planetary Science,* 12B, 262-282.

Jolliff, B.L. (1999) Large-scale separation of K-frac and REEP-frac in the source regions of Apollo impact-melt breccias, and a revised estimate of the KREEP composition. P. 135-154

in *Planetary Petrology and Geochemistry* (eds G.A. Snyder, C.R. Neal, and W.G. Ernst). Bellweather Publishing for Geological Society of America, Washington DC.

Jolliff, B.L., Haskin, L.A., Colson, R.O., and Wadhwa, M. (1993) Partitioning in REE-saturating minerals: Theory, experiment, and modelling of whitlockite, apatite, and evolution of lunar residual magmas. *Geochimica et Cosmochimica Acta,* 57, 4069-4094.

Klemme, S., Günther, D., Hametner, K., Prowatke, S., and Zack, T. (2006) The partitioning of trace elements between ilmenite, ulvospinel, armalcolite and silicate melts with implications for the early differentiation of the Moon. *Chemical Geology,* 234, 251–263.

Korotev, R.L., and Jolliff, B.L. (2001) The curious case of the lunar magnesian granulitic breccias. *Lunar and Planetary Science* XXXII, Abstract 1455.

Korotev R.L., Jolliff B.L., Zeigler R.A., Gillis J.J., and Haskin L.A. (2003) Feldspathic lunar meteorites and their implications for compositional remote sensing of the lunar surface and the composition of the lunar crust. *Geochimica et Cosmochimica Acta,* 67, 4895–4923.

Korzhinskii, D.S. (1965) The theory of systems with perfectly mobile components and processes of mineral formation. *American Journal of Science,* 263, 193-205.

Lindstrom, D.L., and Lindstrom, M.M. (1986) Lunar granulites and their precursor anorthositic norites of the early lunar crust. *Proceedings Of The Sixteenth Lunar And Planetary Science Conference, Part 2; Journal Of Geophysical Research* 91, D263-D276

Liu, Y., Zhang, Y., Rossman, G.R., Eiler, J.M., and Taylor, L.A. (2012) Direct measurement of hydroxyl in the lunar regolith and the origin of lunar surface water. *Nature Geoscience*, 5, 779-782.

LSPET Lunar Sample Preliminary Examination Team (1973) Preliminary Examination of Lunar Samples, Chapter 7 in *Apollo 17 Preliminary Science Report*, NASA SP-330, USGPO.

Lyons, J.I. (1988) Volcanogenic iron oxide deposits, Cerro de Mercado and vicinity, Durango, Mexico. *Economic Geology,* 83, 1886-1906.

Muehlberger, W.R., Batson, R.M., Cernan, E.A., Freeman, V.L., Hait, M.H., Holt, H. E., Howard, K.A., Jackson, E.D., Larson, K.B., Reed, V.S., Rennilson, J.J., Schmitt, H.H., Scott, D.H., Sutton, R.L., Stuart-Alexander, D., Swann, G.A., Trask, N.J., Ulrich, G.E., Wilshire, H.G., and Wolfe, E.W. 1973. Preliminary geologic investigation of the Apollo 17 landing site. In *Apollo 17 Preliminary Science Report.* NASA Special Paper #330. Washington, D.C.: U.S. Government Printing Office. pp. 6-1–6-71.

McCubbin, F.M., Steele, A., Hauri E.H., Nekvasil, H., Yamashita, S., and Hemley, R.J. (2010a) Nominally hydrous magmatism on the Moon. *Proceedings National Academy of Science (USA),* 107, 11223–11228.

McCubbin, F.M., Steele, A., Nekvasil, H., Schnieders, A., Rose, T., Fries, M., Carpenter, P.K., Jolliff, B.L. (2010b) Detection of structurally bound hydroxyl in fluorapatite from Apollo mare basalt 15058,128 using TOF-SIMS. *American Mineralogist* 95, 1141-1150

McCubbin, F.M., Jolliff, B.L., Nekvasil, H., Carpenter, P.K., Zeigler, R.A., Steele, A., Elardo, S.M., and Lindsley, D.H. (2011) Fluorine and chlorine abundances in lunar apatite: Implications for heterogeneous distributions of magmatic volatiles in the lunar interior. *Geochimica et Cosmochimica Acta,* 75, 5073-5093.

McCubbin, F.M., Shearer, C.K., and Sharp, Z.D. (2012) Magmatic volatile reservoirs on the Moon and the chemical signatures of urKREEP. *Second Conference on the Lunar Highlands Crust*, Abstract #9035.

McGee, J.J., Bence, A.E., Eichhorn, G., and Schaeffer, O.A. (1978) Feldspathic granulite 79215: Limitations on T-fO_2 conditions and time of metamorphism. *Proceedings of the 9th Lunar Science Conference*, 743-772.

McKay, D.S., Clanton, U.S., Morrison, D.A., and Ladle, G.H. (1972) Vapor phase crystallization in Apollo 14 breccia. *Proceedings of the Third Lunar Science Conference (Supplement 3, Geochimica et Cosmochimica Acta)* 1, 739-752. The M.I.T. Press.

Meyer, C. (2012) *Lunar Sample Compendium*. http://curator.jsc.nasa.gov/lunar/lsc/index.cfm.

Mittlefehldt, D.W. (1987) Volatile degassing of basaltic achondrite parent bodies: Evidence from alkali elements and phosphorus. *Geochimica et Cosmochimica Acta,* 51, 267-278.

Nash, W.P., and Hausel, W.D. (1973) Partial pressures of oxygen, phosphorus, and fluorine in some lunar lavas. *Earth and Planetary Science Letters*, 20, 13-27.

Neal, C.R., and Taylor, L.E. (1989) Metasomatic products of the lunar magma ocean: The role of KREEP dissemination. *Geochimica et Cosmochimica Acta,* 53, 529-541.

Neal, C.R., and Taylor, L.E. (1991) Evidence for metasomatism of the lunar highlands and the origin of whitlockite. *Geochimica et Cosmochimica Acta,* 55, 2965-2980.

Nekvasil, H., Dondolini, A., Horn, J., Filiberto, J., Long, H., and Lindsley, D.H. (2004) The origin and evolution of silica-saturated alkalic suites: An experimental study. *Journal of Petrology,* 45, 693–721.

557 Nicholis, M.G., and Rutherford, M.J. (2009) Graphite oxidation in the Apollo 17 orange glass
558 magma: Implications for the generation of a lunar volcanic gas phase *Geochimica et*
559 *Cosmichimica Acta,* 73, 5905-5917.
560 Oberli, F., Huneke, J. C., McCulloch, M. T., Papanastassiou, D. A. and Wasserburg, G. J. (1979)
561 Isotopic constraints for the early evolution of the Moon. *Meteoritic*s 14, 502–503
562 Paniello, R.C., Day, J.M.D., and Moynier, F. (2012) Zinc isotopic evidence for the origin of the
563 Moon. Nature 490, 376-379.
564 Pieters, C.M., Goswami, J.N., Clark, R.N., Annadurai, M., Boardman, J., Buratti, B., Combe,
565 J.-P., Dyar, M.D., Green, R., Head, J.W., Hibbitts, C., Hicks, M., Isaacson, P., Klima, R.,
566 Kramer, G., Kumar, S., Livo, E., Lundeen, S., Malaret, E., McCord, T., Mustard, J.,
567 Nettles, J., Petro, N., Runyon, C., Staid, M., Sunshine, J., Taylor, L.A., Tompkins, S., and
568 Varanasi, P. (2009) Character and spatial distribution of OH/H_2O on the surface of the
569 Moon seen by M3 on Chandrayaan-1. *Science*, 326, 568-572.
570 Provencio, P.P., Shearer, C.K., and Brearely, A.J. (2013) Driving fumarole activity on the Moon
571 2: Nano-scale textural and chemical analysis of alteration in "rusty rock" 66095. *Lunar*
572 *and Planetary Science Conference* 44th, Abstract #1669.
573 Reedy, R.C. (1981) Cosmic-ray-produced stable nuclides: Various production rates and their
574 implications. *Proceedings of Lunar and Planetary Science,* 12B, 1809-1823.
575 Rees, C.E., and Thode, H.G. (1974) Sulfur concentrations and isotope ratios in Apollo 16 and 17
576 samples. *Proceedings of the Fifth Lunar Conference (Supplement 5, Geochimica et*
577 *Cosmochimica Acta)* 2, 1963-1973.
578 Robie, R.A., and Hemingway, B.S. (1995) Thermodynamic properties of minerals and related
579 substances at 298.15K and 1 bar (10^5 Pascals) pressure and at higher temperatures. *United*
580 *States Geological Survey Bulletin*, 2131, 461 p.
581 Robinson, K.L., Nagashima, K., and Taylor, G.J. (2013) D/H of intrusive Moon rocks:
582 Implications for lunar origin. *Lunar and Planetary Science Conference 44th*, Abstract
583 #1327.
584 Rumpf, M.E., Fagents S.A., Crawford, I.A. and Joy K.H. (2013) Numerical modeling of lava-
585 regolith heat transfer on the Moon and implications for the preservation of implanted
586 volatiles *Journal of Geophysical Research – Planets,* 118, 382–397.

587 Ruzicka, A., Snyder, G.A., and Taylor, L.A. (2000) Crystal-bearing lunar spherules: Impact
588 melting of the Moon's crust and implications for the origin of meteoritic chondrules.
589 *Meteoritics and Planetary Science,* 35, 173-192.
590 Ryder, G., and Bower, J.F. (1976) Poikilitic KREEP impact melts in the Apollo 14 white rocks.
591 *Proceedings of the 7th Lunar Science Conference*, 1925-1948.
592 Ryder, G., and Martinez, R.R. (1976) Evolved hypabyssal rocks from Station 7, Apennine Front,
593 Apollo 15. *Proceedings Lunar and Planetary Science,* 21, 1925-1948.
594 Saal, A.E., Hauri, E.H., Lo Cascio, M., Van Orman, J.A., Rutherford, M.C., and Cooper, R.F.
595 (2008) Volatile content of lunar volcanic glasses and the presence of water in the Moon's
596 interior. *Nature*, 545, 192-195.
597 Saal, A.E., Hauri, E.H., Van Orman, J.A., and Rutherford, M.C. (2013) Hydrogen isotopes in
598 lunar volcanic glasses and melt inclusions reveal a carbonaceous chondrite heritage.
599 Science, 340, 1317-1320.
600 Salvi, S., and Williams-Jones, A.E. (2006) Alteration, HFSE mineralisation and hydrocarbon
601 formation in peralkaline igneous systems: Insights from the Strange Lake Pluton, Canada.
602 *Lithos,* 91, 19-34.
603 Schmidt, M.W., Dardon, A., Chazot, G., and Vannucci, R. (2004) The dependence of Nb and Ta
604 rutile–melt partitioning on melt composition and Nb/Ta fractionation during subduction
605 processes. *Earth and Planetary Science Letters,* 226, 415– 432.
606 Sharp, Z.D., Shearer, C.K., McKeegan, K.D., Barnes, J.D., and Wang Y.Q. (2010) The chlorine
607 isotope composition of the Moon and implications for an anhydrous mantle. *Science,* 329,
608 1050-1053.
609 Shearer, C.K., Burger, P.V., Papike, J.J., Sharp, Z.D., and McKeegan, K.D. (2011) Fluids on
610 differentiated asteroids: Evidence from phosphates in differentiated meteorites GRA 06128
611 and GRA 06129. *Meteoritics and Planetary Science,* 46, 1345-1362.
612 Shearer, C.K., Sharp, Z.D., McCubbin, F.M., Steele, A., Burger, P.V., Provencio, P.P., and
613 Papike, J.J. (2012a) Chlorine distribution and its isotope composition, alteration mineralogy,
614 and micro-textural analysis of "rusty rock" 66095. Implications for the petrogenesis of
615 "rusty rock", origin of "rusty" alteration, and volatile element behavior on the Moon. *Lunar*
616 *and Planetary Science Conference 43rd*, Abstract #1416.

Shearer, C.K., Burger, P.V., Guan, Y., Papike, J.J., Sutton, S.R., and Atudorei, N.-V. (2012b) Origin of sulfide replacement textures in lunar breccias. Implications for vapor element transport in the lunar crust. *Geochimica et Cosmochimica Acta,* 83, 138-158.

Steefel, C.I., and Maher, K. (2009) Fluid-rock interaction: A reactive transport approach. *Reviews in Mineralogy & Geochemistry,* 70, 485-532.

Tacker, R.C., and Stormer, J.C.Jr. (1993) Thermodynamics of mixing of liquids in the system $Ca_3(PO_4)_2$-$CaCl_2$-CaF_2-$Ca(OH)_2$. *Geochimica et Cosmochimica Acta,* 57, 4663-4676.

Tartese, R., and Anand, M. (2013) Late delivery of chondritic hydrogen into the lunar mantle: Insights from mare basalts. *Earth and Planetary Science Letters*, 361, 480-486.

Tartese, R., Anand, M., Barnes, J.J., Starkey, N.A., Franchi, I.A., and Sano, Y. (2013) The abundance, distribution, and isotopic composition of hydrogen in the Moon as revealed by basaltic lunar samples: Implications for the volatile inventory of the Moon. *Geochimica et Cosmochimica Acta*, 122, 58-74.

Tornabene, L.T., Osinski, G.R., McEwen, A.S., Boyce, J.M., Bray, V.J., Caudill, C.M., Grant, J.A., Hamilton, C.W., Mattson, S., and Mouginis-Mark, P.J. (2012) Widespread crater-related pitted materials on Mars: Further evidence for the role of target volatiles during the impact process. *Icarus,* 220, 348–368.

Treiman, A.H., Maloy, A.K., Shearer, C.K.Jr., and Gross, J. (2010) Magnesian anorthositic granulites in lunar meteorites in lunar meteorites Allan Hills 81005 and Dhofar 309: Geochemistry and global significance. *Meteoritics and Planetary Science,* 45, 163-180.

Wänke, H., Palme, H., Kruse, H., Baddenhausen, H., Cendales, M., Dreibus, G., Hofmeister, H., Jagoutz, E., Palme, C., Spettel, B., and Thacker R. (1976) Chemistry of lunar highland rocks: A refined evaluation of the composition of the primary matter. *Proceedings of the Seventh Lunar Science Conference*, 3479-3499

Warren, P.H., and Wasson, J.T. (1979) The origin of KREEP. *Reviews of Geophysics and Space Physics,* 17, 73-88.

Watson, E.B. (1979) Apatite solubility in basic to intermediate magmas. *Geophysical Research Letters,* 6, 937-940.

Yakovlev, O.I., Dikov, Yu.P., and Gerasimov, M.V. (2006) Experimental data on the thermal reduction of phosphorus and iron and their significance for the interpretation of the impact reworking of lunar materials. *Geochemistry International*, 44, 847-854.

Zhang, Y. (2011) "Water" in lunar basalts: the role of molecular hydrogen (H_2), especially in the diffusion of the H component. *Lunar and Planetary Science Conference 42nd*, Abstract 1957.

COMPETING FINANCIAL INTERESTS

The authors declare that they have no competing interests, or other interests that might be perceived to influence the results and/or discussion reported in this paper.

Correspondence and requests for materials should be addressed to A.H. Treiman.

659 Table 1. Average chemical compositions of minerals, thin section 79215,51.

660

661

	olivine	orthopyroxene	augite	plagioclase	ilmenite
SiO_2	37.93	53.95	51.27	43.85	0.02
TiO_2	0.05	0.59	1.50	0.05	55.77
Al_2O_3	0.06	0.78	2.25	35.02	0.01
Cr_2O_3	0.05	0.37	0.69	0.05	0.33
FeO	24.66	15.08	6.81	0.46	37.68
MnO	0.26	0.26	0.16	0.01	0.40
MgO	36.86	26.97	15.97	0.18	6.39
NiO	0.01	0.01	0.01	0.01	0.01
CaO	0.19	1.79	20.30	18.37	0.07
K_2O	0.00	0.00	0.01	0.68	0.02
Na_2O	0.00	0.00	0.11	0.15	0.00
P_2O_5	0.09	0.01	0.02	0.06	--
Total	100.17	99.84	99.08	98.89	100.68
Normalization					
Cations	3	4	4	5	2
Si	0.997	1.951	1.914	2.047	0.000
Ti	0.001	0.016	0.042	0.002	0.998
Al	0.002	0.033	0.099	1.927	0.009
Cr	0.001	0.011	0.020	0.002	0.006
Fe	0.542	0.456	0.213	0.018	0.749
Mn	0.006	0.008	0.005	0.000	0.008
Mg	1.444	1.454	0.889	0.012	0.226
Ni	0.000	0.000	0.000	0.000	0.000
Ca	0.005	0.069	0.812	0.919	0.002
Na	0.000	0.000	0.000	0.062	0.001
K	0.000	0.000	0.005	0.009	0.000
P	0.002	0.000	0.001	0.002	--
Fo/En/An	72.7	73.5	46.4	92.8	
Fa/Fs/Ab	27.3	23.0	11.1	6.2	
--/Wo/Or		3.5	42.4	0.9	
Chg Imb	0.004	-0.021	0.028	-0.039	0.010

Molar proportions are percentages: for olivine, Fo = Mg/(Mg+Fe) & Fa = Fe/(Mg+Fe); for pyroxenes, En = Mg/(Ca+Mg+Fe), Fs = Fe/(Ca+Mg+Fe), Wo = Ca/(Ca+Mg+Fe); for feldspar, Ab = Na/(Na+Ca+K), An = Ca/(Na+Ca+K), Or = K/(Na+Ca+K). "Chg Imb" is charge imbalance for formula number of oxygens; values near zero imply good stoichiometry.

662
663

Table 2. Chemical composition of apatite in 79215

	*	1 σ*	To 8 cations	
SiO_2	0.41	0.02	Ti	0.001
TiO_2	0.01	0.02	Al	0.001
Al_2O_3	0.01	0.02	Ce	0.002
Ce_2O_3	0.05	0.02	*REE*[a]	*0.012*
REE_2O_3[a]	*0.21*	---	Fe	0.014
FeO	0.20	0.06	Mn	0.002
MnO	0.02	0.02	Mg	0.017
MgO	0.14	0.03	Ca	4.973
CaO	54.86	0.15	*Sr*[b]	*0.002*
SrO[b]	*0.05*	---	Na	0.001
Na_2O	0.01	0.01	K	0.000
K_2O	0.00	0.00	P	2.939
P_2O_5	41.03	0.14	Si	0.002
SO_2	0.03	0.00	S	0.034
F	3.34	0.14	F	0.893
Cl	0.66	0.02	Cl	0.094
OH[c]	0.0025	0.0015	OH[c]	0.0004
O=F,Cl	-1.55	0.06	Charge	
Total	99.46	0.25	Sum	-0.014

*Average of 44 spot EMP analyses; for all analyses, see Deposit Item, Appendix N. [a]Assumes chondritic relative REE abundances (see Fig. 2). [b]Assumes a chondritic Ca/Sr ratio. [c]By ion microprobe, see Table 3. Normalization to 8 total cations gives 5.025 octahedral cations, which ideally should be 5.0, and 0.987 'X' anions, which ideally should be 1.0.

664
665
666

Table 3a. SIMS Data: H_2O Abundance

Analysis	Sample	Grain	$^{16}O^{1}H/^{18}O$	$^{16}O^{1}H/^{18}O$ - blank	1σ	H_2O stds (ppm)	1σ	H2O (ppm)	1σ
Std. SCOL-0328-1	San Carlos	—	0.0028	0	0.00015	0	10	—	
Std. Ap004-0328-1	AP004	—	2.10	2.09	0.00512	5200	100	—	
Std. Ap004-0328-2	AP004	—	1.80	1.80	0.00350	5200	100	—	
Std. Ap003-0328-1	AP003	—	0.17	0.17	0.00080	340	100	—	
Std. Ap003-0328-2	AP003	—	0.16	0.16	0.00105	340	100	—	
Std. Ap005-0328-1	AP005	—	1.04	1.04	0.00333	3900	100	—	
Std. Ap005-0328-2	AP005	—	1.28	1.28	0.00476	3900	100	—	
OH-79215-51-Ap3-1	79215	AP3	0.0065	0.00374	0.00020	—	—	19	
OH-79215-51-Ap2-3	79215	AP2	0.0075	0.00472	0.00016	—	—	22	
OH-79215-51-Ap1-1	79215	AP1	0.0125	0.00966	0.00026	—	—	36	
OH-79215-51-Ap1-1@1	79215	AP1	0.0083	0.00555	0.00014	—	—	24	
Std. 79215-51-OL@1	79215	OL1	0.0088	0.00605	0.00015	—	—	25	
Std. 79215-51-OL@2	79215	OL1	0.0062	0.00336	0.00014	—	—	18	
Std. 79215-51-OL@3	79215	OL1	0.0069	0.00413	0.00012	—	—	20	
Std. 79215-51-OL@4	79215	OL1	0.0071	0.00435	0.00011	—	—	20	
Std. 79215-51-Plag@1	79215	P2	0.0033	0.00053	0.00013	—	—	9	
79215 Apatite average	**79215**		**0.00871**	**0.00591**				**25.0**	**7.6**

Table 3b. SIMS: Deuterium / Hydrogen Ratio.

Analysis name	Sample	Grain	$^{2}H/^{1}H$	1σ	δD raw	1σ	δD Corrected	1σ
Std. DH_FA4_durango@1	Durango	—	9.44E-05	4.32E-06	-394	28	—	—
Std. DH_FA4_durango@2	Durango	—	9.29E-05	4.89E-06	-403	31	—	—
Std. DH_FA4_durango@2b	Durango	—	1.02E-04	3.70E-06	-343	24	—	—
Std. DH_FA4_durango@1b	Durango	—	1.05E-04	3.53E-06	-326	23	—	—
79215 DH-Ap2-6	79215	AP2	2.48E-04	1.44E-05	592	93	1082	93
79215 DH-Ap4-1	79215	AP4	2.66E-04	1.62E-05	709	104	1234	104
79215 DH-Ap4-2	79215	AP4	2.16E-04	1.12E-05	385	72	811	78
79215 DH-Ap4-3	79215	AP4	2.50E-04	7.46E-06	607	48	1101	78
Std. DH_FA4_durango@3	Durango	—	9.19E-05	1.54E-06	-410	10	—	—
Std. DH_FA4_durango@4	Durango	—	1.05E-04	2.48E-06	-325	16	—	—
Std. DH_FA4_durango@5	Durango	—	1.33E-04	2.29E-06	-143	15	—	—
Std. DH_FA4_durango@6	Durango	—	1.13E-04	1.82E-06	-276	12	—	—
Std. DH_FA4_durango@7	Durango	—	1.06E-04	3.01E-06	-320	19	—	—
Std. DH_FA4_durango@8	Durango	—	1.14E-04	4.58E-06	-266	29	—	—
Std. DH_FA4_durango@8b	Durango	—	9.50E-05	1.62E-06	-390	10	—	—
79215 Apatite average	**79215**		**2.45E-04**	**1.23E-05**	**573**		**1057**	**88**

Table 3c. SIMS: Chlorine Abundances.

Analysis	Sample	Grain	$^{35}Cl/^{18}O$	$^{35}Cl/^{18}O$ - blank	1σ	Cl stds	1σ	Cl (ppm)
Std. SCOL-0328-1	San Carlos	—	5.35E-04	0.00E+00	4.78E-05	0	10	—
Std. Ap004-0328-1	AP004	—	6.35	6.35	0.02	4100	100	—
Std. Ap004-0328-2	AP004	—	5.92	5.92	0.01	4100	100	—
Std. Ap003-0328-1	AP003	—	6.38	6.38	0.03	4500	100	—
Std. Ap003-0328-2	AP003	—	5.84	5.84	0.02	4500	100	—
Std. Ap005-0328-1	AP005	—	11.42	11.42	0.04	9500	100	—
Std. Ap005-0328-2	AP005	—	12.11	12.11	0.02	9500	100	—
OH-79215-51-Ap3-1	79215	AP3	10.34	10.34	0.03	—	—	7949
OH-79215-51-Ap2-3	79215	AP2	10.86	10.86	0.02	—	—	8342
OH-79215-51-Ap1-1	79215	AP1	10.81	10.81	0.03	—	—	8307
OH-79215-51-Ap1-1@1	79215	AP1	10.95	10.95	0.02	—	—	8414
Std. 79215-51-OL@1	79215	OL1	4.66E-04	-6.95E-05	3.91E-05	—	—	~0
Std. 79215-51-OL@2	79215	OL1	3.75E-04	-1.61E-04	3.37E-05	—	—	~0
Std. 79215-51-OL@3	79215	OL1	3.75E-04	-1.61E-04	2.35E-05	—	—	~0
Std. 79215-51-OL@4	79215	OL1	4.21E-04	-1.15E-04	3.81E-05	—	—	~0
Std. 79215-51-Plag@1	79215	P2	4.39E-04	-9.58E-05	4.93E-05	—	—	~0
79215 Apatite average	**79215**		**10.74**	**10.74**	**0.02798**		**207**	**8253**

676

677 Table 3d. SIMS: Chlorine Isotope Ratios.

Analysis	Sample	Grain	$^{37}Cl/^{35}Cl$	1σ	raw $\delta^{37}Cl$	corrected $\delta^{37}Cl$	1σ
Std. Durango_0326@1	Durango	—	0.3189	0.00017	-2.6	-0.9	1.1
Std. Durango_0326@2	Durango	—	0.3191	0.00022	-2.1	-0.3	1.1
Std. Durango_0326@3	Durango	—	0.3187	0.00017	-3.4	-1.7	1.1
Std. Durango_0326@4	Durango	—	0.3193	0.00014	-1.3	0.4	1.1
Std. Durango_0326@5	Durango	—	0.3196	0.00020	-0.4	1.3	1.1
Std. Durango_0326@6	Durango	—	0.3198	0.00021	0.0	1.7	1.1
Std. Durango_0326@7	Durango	—	0.3191	0.00017	-2.0	-0.2	1.1
Std. Durango_0326@8	Durango	—	0.3192	0.00020	-1.8	-0.1	1.1
79215-51-Ap3-1	79215	AP3	0.3295	0.00011	30.6	32.4	1.1
79215-51-Ap3-1b	79215	AP3	0.3300	0.00014	32.2	33.9	1.1
79215-51-Ap3-2	79215	AP3	0.3300	0.00015	32.0	33.8	1.1
79215-51-Ap2-1	79215	AP2	0.3293	0.00021	29.8	31.6	1.1
79215-51-Ap2-2	79215	AP2	0.3295	0.00016	30.3	32.1	1.1
79215-51-Ap2-3	79215	AP2	0.3294	0.00014	30.1	31.9	1.1
79215-51-Ap2-4	79215	AP2	0.3296	0.00017	30.7	32.5	1.1
79215-51-Ap2-4b	79215	AP4b	0.3298	0.00011	31.5	33.3	1.1
Std. Durango_0327@1	Durango	—	0.3195	0.00014	-0.7	1.0	1.1
Std. Durango_0327@2	Durango	—	0.3195	0.00019	-0.7	1.0	1.1
Std. Durango_0327@3	Durango	—	0.3195	0.00013	-0.9	0.9	1.1
Std. Durango_0327@4	Durango	—	0.3198	0.00014	0.1	1.8	1.1
79215-51-Ap1-1	79215	AP1	0.3297	0.00012	31.2	33.0	1.1
79215-51-Ap1-2	79215	AP1	0.3295	0.00008	30.6	32.3	1.1
79215-51-Ap5a-1	79215	AP5a	0.3297	0.00015	30.9	32.7	1.1
79215-51-Ap5a-2	79215	AP5a	0.3299	0.00016	31.7	33.5	1.1
79215-51-Ap5b-2	79215	AP5a	0.3293	0.00015	29.7	31.5	1.1
79215 Apatite average	**79215**		**0.3296**		**30.9**	**32.7**	**0.8**

678

679 Table 3e. SIMS: Sulfur Abundances.

Analysis name	Sample	Grain	$^{32}S/^{18}O$	$^{32}S/^{18}O$-blank	1σ	S stds	1σ	S (ppm)
Std. SCOL-0328-1	San Carlos	—	0.00031	0.00000	0.00004	0	10	—
Std. Ap004-0328-1	AP004	—	2.44	2.44035	0.00908	1005	100	—
Std. Ap004-0328-2	AP004	—	2.27	2.27014	0.00424	1005	100	—
Std. Ap003-0328-1	AP003	—	2.57	2.56512	0.00728	1262	100	—
Std. Ap003-0328-2	AP003	—	2.37	2.36726	0.00810	1262	100	—
Std. Ap005-0328-1	AP005	—	0.78	0.77716	0.00326	407	100	—
Std. Ap005-0328-2	AP005	—	0.81	0.80973	0.00239	407	100	—
OH-79215-51-Ap3-1	79215	AP3	0.23	0.22620	0.00110	—	—	111
OH-79215-51-Ap2-3	79215	AP2	0.22	0.21785	0.00092	—	—	107
OH-79215-51-Ap1-1	79215	AP1	0.21	0.20840	0.00106	—	—	103
OH-79215-51-Ap1-1@1	79215	AP1	0.21	0.20731	0.00121	—	—	102
Std. 79215-51-OL@1	79215	OL1	0.00032	0.00001	0.00004	—	—	~0
Std. 79215-51-OL@2	79215	OL1	0.00016	-0.00014	0.00002	—	—	~0
Std. 79215-51-OL@3	79215	OL1	0.00021	-0.00009	0.00002	—	—	~0
Std. 79215-51-OL@4	79215	OL1	0.00017	-0.00013	0.00003	—	—	~0
Std. 79215-51-Plag@1	79215	P2	0.00018	-0.00013	0.00003	—	—	~0
79215 Apatite average	**79215**		**0.21525**	**0.21494**	**0.0011**			**106**

680

681 Table 3f. SIMS: Sulfur Isotope Ratios.

Analysis	Sample	Grain	$^{33}S/^{32}S$	1σ	$^{34}S/^{32}S$	1σ	$\delta^{33}S$	1σ	$\delta^{34}S$	1σ
Std. Durango@10	Durango	—	0.0079113	1.041E-05	0.0446281	5.993E-05	4.4	1.3	10.5	1.4
Std. Durango@11	Durango	—	0.0078941	9.203E-06	0.0445182	4.127E-05	2.2	1.2	8.0	0.9
Std. Durango@12	Durango	—	0.0079003	8.265E-06	0.0445265	4.046E-05	3.0	1.0	8.2	0.9
Std. Durango@13	Durango	—	0.0078926	1.013E-05	0.0444468	5.307E-05	2.0	1.3	6.4	1.2
Std. Durango@14	Durango	—	0.0079048	7.247E-06	0.0446093	4.568E-05	3.5	0.9	10.2	1.0
79215-51-S-Ap2-5	79215	AP2	0.0079185	1.607E-05	0.0446615	6.704E-05	5.3	2.0	11.3	1.5
79215-51-S-Ap2-6	79215	AP2	0.0079218	1.158E-05	0.0445912	6.257E-05	5.7	1.5	9.7	1.4
Std. Durango@15	Durango	—	0.0079205	6.673E-06	0.0445360	4.597E-05	5.5	0.8	8.4	1.0
Std. Durango@16	Durango	—	0.0079034	7.464E-06	0.0444470	4.696E-05	3.4	0.9	6.4	1.1
Std. Durango@17	Durango	—	0.0079330	8.843E-06	0.0444632	5.603E-05	7.1	1.1	6.8	1.3
Std. Durango@18	Durango	—	0.0078981	9.149E-06	0.0443730	5.840E-05	2.7	1.2	4.7	1.3
Std. Durango@19	Durango	—	0.0079113	1.041E-05	0.0444304	7.529E-05	3.4	1.6	6.0	1.7
Std. Durango@20	Durango	—	0.0079112	1.108E-05	0.0444679	6.435E-05	4.3	1.4	6.9	1.5
Std. Durango@21	Durango	—	0.0078997	9.470E-06	0.0443659	6.482E-05	2.9	1.2	4.6	1.5
Std. Durango@22	Durango	—	0.0078991	9.504E-06	0.0445196	3.948E-05	2.8	1.2	8.1	0.9
Std. Durango@23	Durango	—	0.0079170	7.890E-06	0.0445737	3.840E-05	5.1	1.0	9.3	0.9
Std. Durango@24	Durango	—	0.0079119	8.412E-06	0.0444635	3.836E-05	4.4	1.1	6.8	0.9
79215 Apatite average	**79215**		**0.0079201**	**0.000014**	**0.0446263**	**0.000065**	**5.5**	**1.8**	**10.5**	**1.5**

682

683

Table 4. Mineralogy & Chemistry of Magnesian Feldspathic Granulites.

Sample	% plagioclase	Mg#	% apatite*	% merrillite*	ppm La‡
79215	82	77	~1	0	2.7
15418	70	65	--	--	1.8
67415	~80	78	--	--	4.4
67955	75	80	--	--	4.6
72559	75	80	--	--	3.3
76235	70	75	--	--	3.0
77017	75	70	--	--	4.2
78155	75	65	--	tr	4.0

Data from compilation of Meyer (2012). Modal (volume) proportions of minerals. Mg# is molar Mg/(Mg+Fe) in mafic minerals. * 'tr' = trace proportions (<0.1%) reported. '--' = none reported. ‡ Average La abundance as a measure of KREEP content – values < ~10 ppm imply minimal REE from a KREEP component.

a.

2 mm

b.

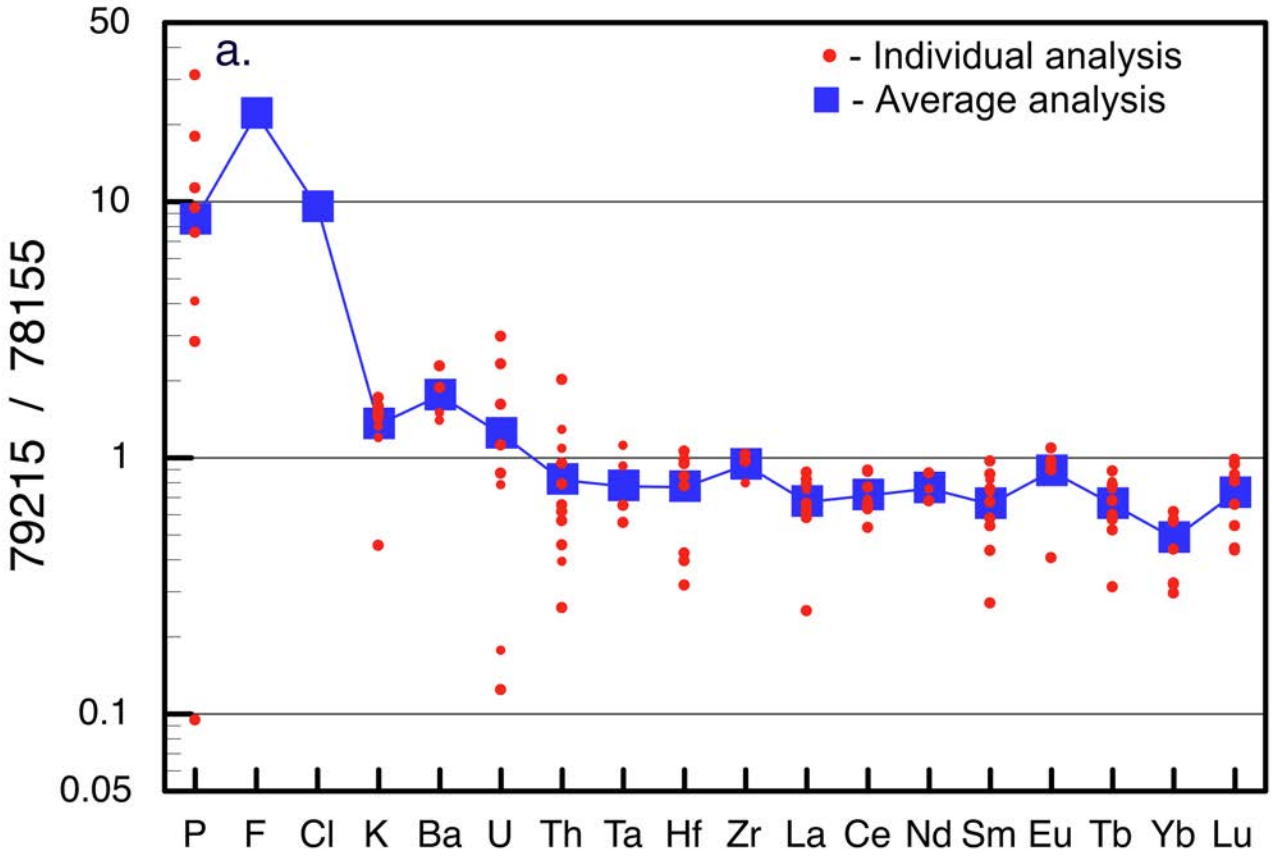
a.
- Individual analysis
- Average analysis
79215 / 78155
50
10
1
0.1
0.05
P F Cl K Ba U Th Ta Hf Zr La Ce Nd Sm Eu Tb Yb Lu

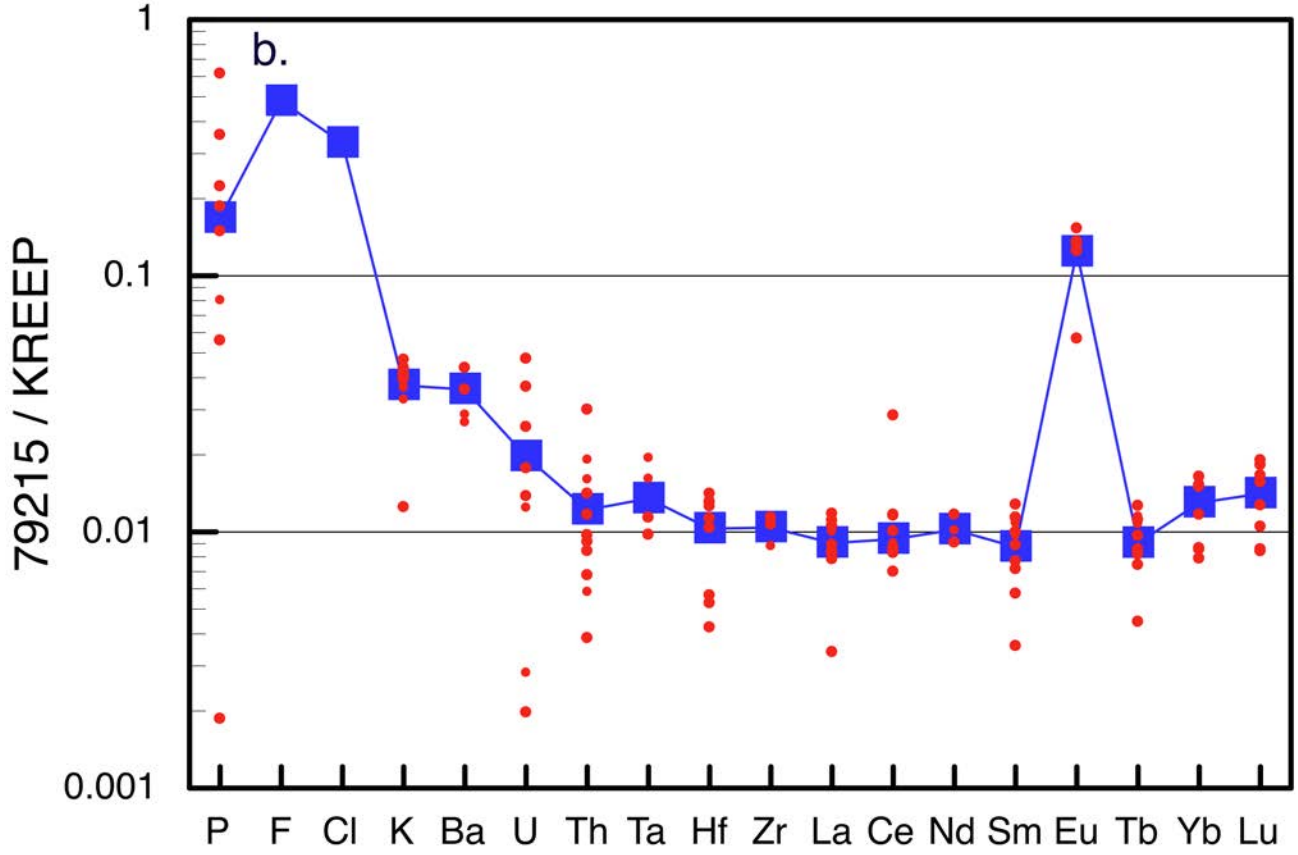
b.
79215 / KREEP
1
0.1
0.01
0.001
P
F
Cl
K
Ba
U
Th
Ta
Hf
Zr
La
Ce
Nd
Sm
Eu
Tb
Yb
Lu

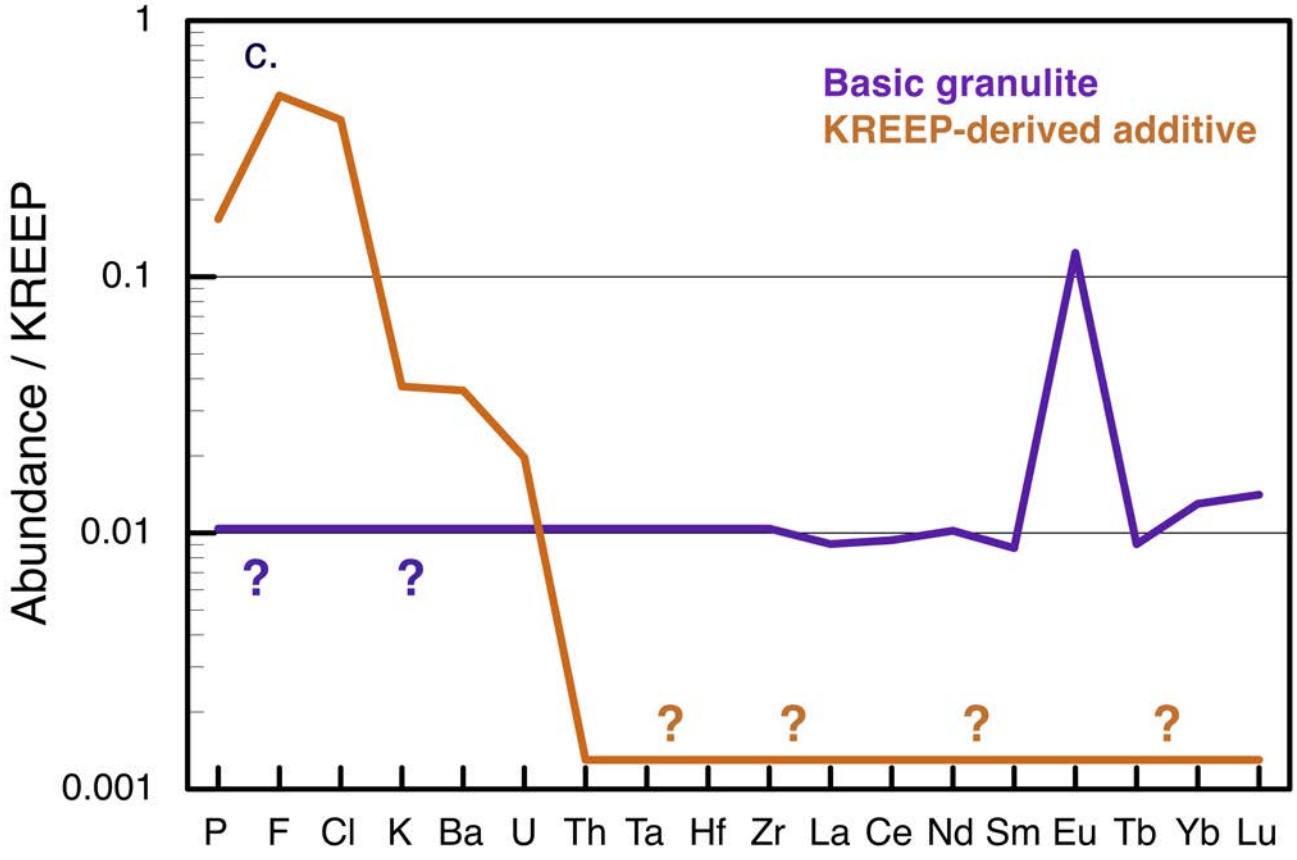
c.
Basic granulite
KREEP-derived additive
Abundance / KREEP
1
0.1
0.01
0.001
?
?
?
?
?
?
P F Cl K Ba U Th Ta Hf Zr La Ce Nd Sm Eu Tb Yb Lu

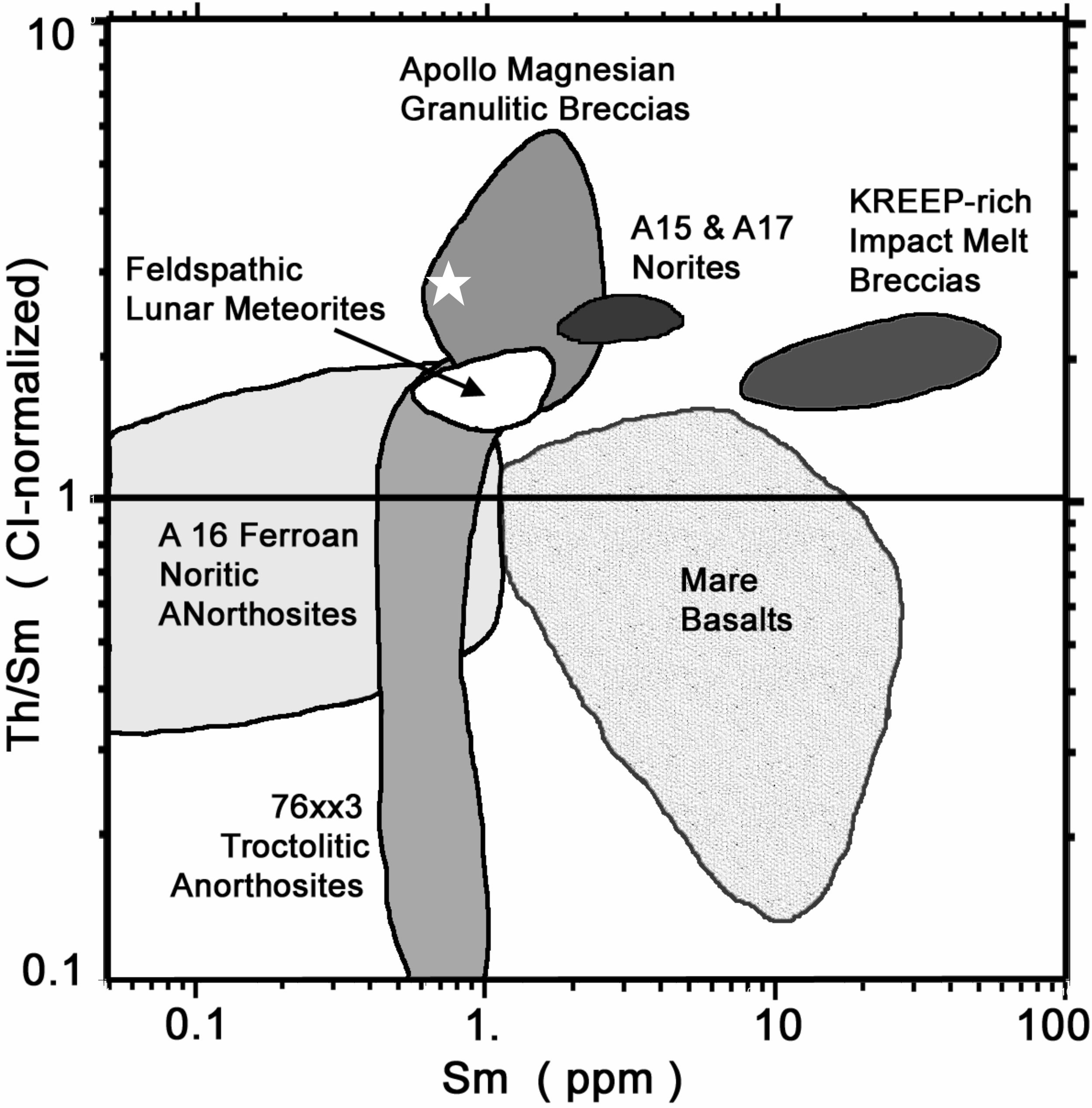
10
1
0.1
(Cl-normalized)
Th/Sm
Apollo Magnesian
Granulitic Breccias
A15 & A17
Norites
KREEP-rich
Impact Melt
Breccias
Feldspathic
Lunar Meteorites
A 16 Ferroan
Noritic
ANorthosites
Mare
Basalts
76xx3
Troctolitic
Anorthosites
0.1
1.
10
100
Sm (ppm)